# Multiscale Community Detection in Functional Brain Networks Constructed Using Dynamic Time Warping

Di Jin, Rui Li, and Junhai Xu

***Abstract*— Previous studies have focused on the detection of community structures of brain networks constructed with resting-state functional magnetic resonance imaging (fMRI) data. Pearson correlation is often used to describe the connections between nodes in the construction of functional brain networks, which typically ignores the inherent timing and validity of fMRI time series. To solve this problem, this study applied the Dynamic Time Warp (DTW) algorithm to determine the correlation between two brain regions by comparing the synchronization and asynchrony of the time series. In addition, to determine the best community structure for each subject, we further divided the brain network into different scales, and then detected the different communities in these brain networks by using Modularity, Variation of Information (VI) and Normalized Mutual Information (NMI) as structural monitoring variables. Finally, we affirmed each subject's best community structure based on them. The experiments showed that through the method proposed in this paper, we not only accurately discovered important components of seven basic functional subnetworks, but also found that the putamen and Heschl's gyrus have a relationship with the inferior parietal network. Most importantly, this method can also determine each subject's functional brain network density, thus confirming the findings of studies testing real brain networks.**

***Index Terms*— DTW, multiscale, community detection.**

## I. Introduction

THE functional system of the human brain is thought to involve a complex network with interconnected, interacting components [1]. Like many realistic networks in nature and society, the brain network is characterized by its community structure [2]. Specifically, communities are groups of nodes forming tightly connected units that are only weakly linked to each other. It has been shown that there are some important communities in the brain network, such as the visual [3], auditory [4], language [5], and other communities. These reflect topological relationships between elements of the underlying system and represent functional entities, which are critical for researching the emergence of adaptive behaviors and cognition. Generally, such functional brain community structures can be revealed by using the resting-state functional magnetic resonance imaging (fMRI), and these communities are also known as resting-state sub-networks [6]. Community detection in functional brain networks facilitates the understanding of the underlying brain organization and its related cognitive function [7]. Detecting the community structure is one of the most important issues in exploring the architecture of our human brain.

Many techniques at present have been proposed for detecting community structure of the functional brain network. Technically, when building a brain network using imaging data, the first step is typically to define the nodes and then estimate links between them [8]. The nodes represent disjointed brain regions and the links reflect the correlation between different brain regions. Generally, the use of fixed spatial regions of interest (ROIs) assessed by anatomical atlases is one of the most popular methods for defining brain nodes [9]. In addition, link weights are defined as interregional temporal correlations in the fluctuations of the Blood Oxygen Level Dependent (BOLD) signals, and the resulting network can be represented by a correlation adjacency matrix [10]. Currently, a series of approaches have been proposed to define the links, of which the Pearson correlation is the simplest and most popular way [11]. Although it has been successfully applied to the estimation of functional connectivity, the Pearson correlation only measures the correlation between nodes based on the synchronization principle of low frequency signals. Partial correlation analysis has been further developed to calculate the correlation of low-frequency signals without the influence of other variables [12]. However, both Pearson correlation and Partial correlation can only capture low-order statistics by calculating the pairwise correlation between distinct brain nodes [13]. In practice, synchronization and asynchronism of higher BOLD signals may also offer additional and useful information for the analysis of functional connectivity [14]–[16]. Therefore, retaining the low-frequency and high-frequency information of BOLD signals is of great significance and can make the functional brain network much closer to a real brain. In addition, we need to detect communities in functional brain networks. According to

Manuscript received February 28, 2019; revised June 21, 2019, September 1, 2019, and October 10, 2019; accepted October 14, 2019. Date of publication October 17, 2019; date of current version January 8, 2020. This work was supported by the National Natural Science Foundation of China under Grant 61703302 and Grant 61772361. *(Corresponding author: Junhai Xu.)*

The authors are with the Tianjin Key Laboratory of Cognitive Computing and Application, College of Intelligence and Computing, Tianjin University, Tianjin 300350, China (e-mail: jindi@tju.edu.cn; lirui940301@163.com; jhxu@tju.edu.cn).

This article has supplementary downloadable material available at http://ieeexplore.ieee.org, provided by the author.

Digital Object Identifier 10.1109/TNSRE.2019.2948055

a recent study [17], it is most reasonable to define about 260 links in a functional brain network with 90 nodes, which means that the network density value is around 5.8%. According to this, a weighted network is often transformed into a dichotomous network. However, there are individual differences in network density, which means that the density of functional brain network varies from person to person. Previous studies have shown that an individual's functional brain connectivity profile is both unique and reliable [18]. The classical techniques of network density selection based on experience alone cannot reflect this characteristic. Determining the functional brain network density is of great significance to the study of individual differences such as intelligence, brain diseases and so on [19]. At present, to determine the optimal brain network desity, the study divided the brain network into different scales using dichotomy and then detected the community structures in these brain networks and selected reasonable thresholds based on modularity. Density selection has a significant impact on the study of brain function [20], [21]. However, there are limitations when using modularity alone because of the resolution limit and the degeneracy of near-optimal solutions [22]. It is difficult to obtain an optimal solution if only the value of the modularity is used.

To address the above issues, this study put forward a method to analyze the synchronization and asynchronism of fMRI time series based on Dynamic Time Warping (DTW). Dinov et al in 2016 applied DTW measures in EEG and fMRI datasets and found that predictability is almost always higher in tasks than in rest states compared with standard discrete Fourier transform, which provided additional evidence for the utility of the DTW approach in neuroscience [23]. Furthermore, Meszlényi et al in 2017 used DTW to evaluate functional connectivity strength and proved that DTW is less sensitive to linearly combined global noise in the data as compared to traditional correlation analysis [24].Therefore, DTW has great significance in exploring neuroscience. In this paper, we use DTW to construct functional brain network and found that its network characteristics are better than other networks' characteristics constructed by traditional methods, like Pearson correlation and Partial correlation. To further prove that DTW network is closer to a real brain network, we detect communities in different functional brain network based on different methods. In addition, new measures, the Variation of Information (VI) [25] and the Normalized Mutual information (NMI) [26] are proposed along with modularity as criteria for examining the best community structure of the binary network. In this case, a reasonable threshold can be determined, and a stable community structure can be identified for each subject. Finally, with the method proposed in this study, seven basic brain networks were discovered, and a new network in the inferior parietal lobe was observed. The main contributions of this study can be summarized as follows:

(1) The study applies the DTW technique to construct functional brain networks. The functional brain network constructed by DTW showed a more obvious "small-world" effect [27] than that using Pearson correlation and Partial correlation. This can help us to better study the community structure of the functional brain network.

(2) For the functional brain network constructed using DTW, modularity, VI and NMI were used as criteria to measure the stability of the community structure. This will allow not only the identification of the best community structure for each subject, but also the determination of network density.

(3) Using our method, we have accurately observed the main components of seven basic communities. More importantly, a new subnetwork in the inferior parietal network was discovered, which also included the putamen, Heschl's gyrus, the angular gyrus and the supramarginal gyrus.

## II. Data Acquisition and Preprocessing

### A. Experimental Data Set

An open resting-state functional magnetic resonance imaging (fMRI) dataset was used in this study http://www.nitrc.org/projects/nyu_trt/. In the experiment, twenty-five participants (mean age, 29.4 $\pm$ 8.6 years, 10 males) were scanned for three times. Participants were confirmed by a clinical assessment without history of mental illness or neurological diseases. Participants were informed and agreed before participating. The data collection was approved by the Institutional Review Committee of New York University and New York University Medical School.

### B. fMRI Data Acquisition

All data were collected on a Siemens 3T Tim Trio scanners (Siemens, Erlangen, Germany). For the core data set, subjects were instructed to remain still, stay awake, and keep their eyes open. All participants were scanned three times. A software upgrade (VB15 to VB17) occurred on all scanners during the study. Validation studies that acquired structural and functional data on the same individuals before and after the upgrade could not detect an effect of the upgrade. The functional imaging data were acquired using a gradient-echo echo-planar imaging (EPI) sequence with the following parameters: repetition time (TR) = 2000 ms; echo time (TE) = 25 ms; flip angle = 90°, 39 slices, matrix = 64 $\times$ 64; field of view (FOV) = 192 mm; acquisition voxel size = $3 \times 3 \times 3\ mm^3$. Scans 2 and 3 were obtained in a single scan session, 45 min apart, between 5 and 16 months (mean, 11 $\pm$ 4 months) after scan 1. Whole brain coverage including the entire cerebellum was achieved with slices aligned to the anterior commissure-posterior commissure plane using an automated alignment procedure, ensuring consistency among subjects. For spatial normalization and localization, a high-resolution T1-weighted magnetization prepared gradient echo sequence was also obtained (TR = 2500 ms; TE = 4.35 ms; TI = 900 ms; flip angle = 8°; 176 slices, FOV = 256 mm).

### C. fMRI Data Preprocessing

The fMRI data were preprocessed with a series of steps common to fMRI analyses. Data preprocessing involves (1) discarding of the first four volumes of each run to allow for T1-equilibration effects, (2) compensating for slice acquisition-dependent time shifts per volume (3) correcting for

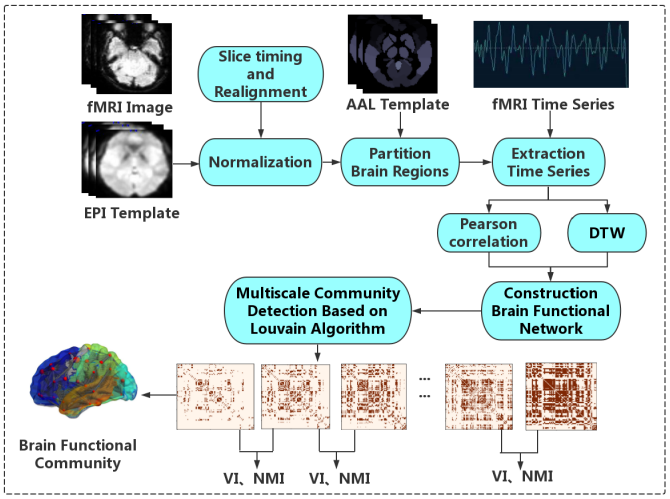


Fig. 1. Flowchart of this study. First, the input fMRI image is preprocessed, including slice timing, realignment and normalization. Second, the time series of each region were extracted according to the AAL template. Then, different functional brain networks were constructed, based on Pearson correlation and Dynamic Time Warping (DTW). Finally, the Louvain algorithm was applied to detect the communities of the functional brain networks under different scales. The Variation of Information (VI) and Normalized Mutual information (MNI) were used to discover the best results using the multiscale community detection.

head motion using rigid body translation and rotation. All subjects' head motion was less than 1.5 mm. In this study, image preprocessing was carried out using the statistical parametric mapping (SPM12, http://www.fil.ion.ucl.ac.uk/spm/) software package. The corrected images were spatially normalized to the Montreal Neurological Institute (MNI) EPI template in SPM12 and resampled to 3 mm cubic voxels.

This study included 25 subjects. the human brain was divided into 116 brain regions by using the Automated Anatomical Labeling (AAL) template atlas [28] provided by the Montreal Neurological Institute (MNI), in which the cerebral cortex was divided to 90 regions, and the cerebellum consists of 26 regions. The fMRI time series of each brain region was extracted and sampled with 220 time points. In order to determine the commonness of the human brain and construct a network closer to that of a real brain, this study calculated the average time series of the corresponding brain regions of 25 subjects.

## III. Methods

### A. Overview

Because of differences in brain structure and function, the optimal network density varies among individuals. It is helpful for the analysis of individual differences to identify the best community structure using multiscale community detection. First, based on the node (brain region) defined in the second part, this study uses DTW as a new criterion to measure the similarity between nodes. Then, we divided the functional brain networks into communities of different scales using the well-known Louvain algorithm [29]. Finally, we introduced the Variation of Information (VI) and modularity as structural monitoring variables to examine the optimal community division. The flowchart of this study is shown in Figure 1.

### B. Construction of Functional Brain Networks

In this section, we introduce the methods associated with function connectivity, including Pearson correlation, Partial correlation and the Dynamic Time Warping.

*1) Baseline Methods:* Pearson correlation and Partial correlation are both measures of linear dependence between two signals. Function connectivity based on Pearson correlation is defined as follows:

$$P = \frac{(x_i - \overline{x_i})^T (x_j - \overline{x_j})}{\sqrt{(x_i - \overline{x_i})^T (x_i - \overline{x_i})}\sqrt{(x_j - \overline{x_j})^T (x_j - \overline{x_j})}}$$

where $x_i \in R^N (i = 1, 2, \ldots\ldots, p)$ is the time series associated with the $i$th ROI, $N$ is the total number of temporal image volumes, $P$ is the number of ROIs, and $\overline{x_i} \in R^N (i = 1, 2, \ldots\ldots, p)$ is the corresponding mean vector of $x_i$. Partial correlation analysis is further developed on the basis of Pearson correlation, which excludes the influence of other variables [29]. In other words, when two variables are correlated with a third variable, the relationship between the two variables cannot be accurately reflected based on the correlation coefficient of the two variables. Therefore, the Partial correlation coefficient is a more accurate method to calculate the community between two variables. The covariance matrix and its inverse matrix are obtained by the correlation matrix:

$$X = Cov(P)$$
$$p = (p_{ij}) = (X)^{-1}$$

where $X$ is the covariance matrix of all the variables and $P$ the inverse of the covariance matrix. The partial correlation matrix can be calculated as:

$$Y_{ij} = -\frac{r_{ij}}{\sqrt{r_{ii} r_{jj}}}$$

$Y_{ij}$ means the correlation between the $i$th ROI and the $j$th ROI, the greater the value of $Y_{ij}$, the closer the connection between two ROIs.

*2) The Proposed Method:* Obviously, when using Pearson correlation and Partial correlation it is possible to simultaneously compare the time series (see Figure 2 A(a)). DTW can solve this discrepancy and calculate the matching distance by recovering the optimal alignments between time points in the two time series. In this case, it reflects the asynchronism between brain regions. The alignment is optimal in the sense that it minimizes the cumulative distance measure consisting of "local" distances between aligned time series, as shown in Figure 2 B(a). First, we define a distance matrix $d = (d_{ij})$ representing the time distance between different ROIs.

$$d_{ij}(b, k) = |B(N_i, T_b) - B(N_j, T_k)|$$
$$1 \le i, \quad j \le 116, \ i \ne j, \ 1 \le b, \ k \le 220$$

where $B(N, T)$ represents each participant's fMRI time series of the corresponding brain regions, where $T_i \in T^N (i = 1, 2, \ldots\ldots, 220)$ is the $i$th time point associated with the $N$th (N = 1, 2, . . . . ., 116) ROI. Then, it warps the time axes of the two time series in such a way that the corresponding samples appear at the same location on a common time axis. The DTW-distance between two time series is $D_{ij}(M, N)$, which

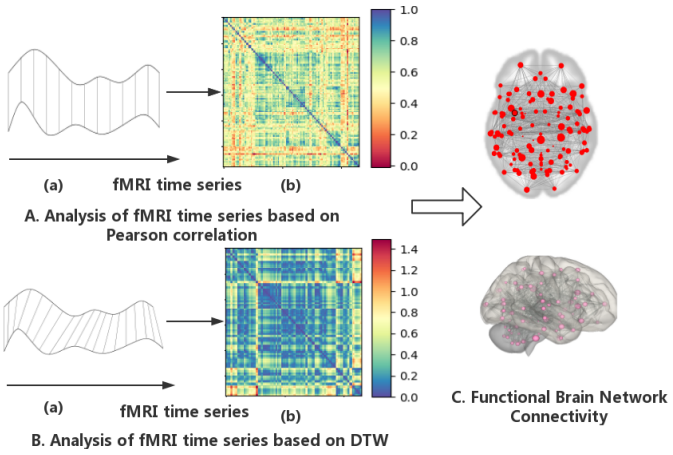


Fig. 2. Functional connectivity process. (a) both A and B represent the similarity of the fMRI time series using two intuitive methods. (b) in A the similarity matrix based on Pearson correlation is visualized; the larger the values of the color bar, the more similar the ROIs are. (b) in B the loss matrix based on the DTW is visualized; a smaller value means a higher similarity. (c) denotes connections between different brain regions in the functional brain network.

can be calculated using a dynamic programming approach using:

$$D_{ij}(m,n) = \begin{cases} d_{ij}(m,n) + D_{ij}(m,n-1), & if(m=1, n>1) \\ d_{ij}(m,n) + D_{ij}(m-1,n), & if(m>1, n=1) \\ d_{ij}(m,n), & if(m=1, n=1) \\ d_{ij}(m,n) + min\{D_{ij}(m-1,n-1), D_{ij}(m \\ \quad -1,n), D_{ij}(m,n-1)\}, & if(m,n>1) \end{cases}$$

where $1 \le n, m \le 220$, M,N represent the sets of fMRI time points ($n \in N, m \in M$), backtracking along the minimum cost index pairs $(m,n)_k$ starting from $(M,N)$ yields the DTW warping path. The minimum cumulative distance along the path indicates the loss of two brain regions as follows:

$$L(i,j) = D_{ij}(220,220)$$

The greater the $L_{ij}$ value, the smaller the similarity between the two brain regions, and the smaller the $L_{ij}$ value, the greater the similarity between the two brain regions, as shown in Figure 2.

### C. Characteristics of the Constructed Functional Brain Network

In order to compare the functional brain networks constructed by the three different methods, the characteristics of the brain networks were calculated. Previous studies have shown that the functional brain network has a "small world" effect. It is characterized by a clustering coefficient and an average shortest path length [30]. Specifically, local clustering or cliquishness of the connections between neighboring nodes is dense, while the path length between any (distant) pair of nodes is shorter due to the existence of relatively few long-range connections. To prove this, we analyzed the functional brain networks based on different methods using the clustering coefficient $C$ and the average shortest path length $L$. We calculated the values of $C$ and $L$ for the functional brain network, as well as the $C_{rand}$ and $L_{rand}$ of a random network at the same scale. When the clustering coefficient ratio of the same scale brain function network and the random network is $\gamma = C/C_{rand} > 1$, the average shortest path length ratio is $\lambda = L/L_{rand} \sim 1$. Small-worldness can be depicted by $\sigma = \gamma/\lambda > 1$, if the value obtained is $>1$, then the network is considered to have a small world effect.

### D. Community Detection in Functional Brain Networks

In order to determine the best network density for an individual, this study uses dichotomy to determine different thresholds for the observation of the community structures of the brain networks at different densities, and then identify highly stable community structures. This study analyzes the functional brain networks with different densities by assigning the brain regions whose loss is less than the threshold value of 1 and assigning the brain regions whose similarity is greater than the threshold value of 0. Since the number of brain function links is unknown, it is necessary to divide the adjacency matrices at different densities and determine the best community structure under each density, so that each point in the community is closely connected, while the connections between different communities are relatively sparse. In order to quantify this concept, Newman and Girvan [31] put forward the concept of modularity in 2004:

$$Q = \frac{1}{2m}\sum_{ij}\left(A_{ij} - \frac{k_i k_j}{2m}\right)\delta(C_i, C_j)$$

where the adjacency matrix $A = \{a_{ij}\}$ of a binary network is a square $n \times n$ symmetric matrix with elements $A_{ij} = 1$ when an link exists between node $i$ and $j$ and 0 otherwise. $k_i$ represents the degree of the node $i$, $\delta(C_i, C_j)$ is defined as follows:

$$\delta(C_i, C_j) = \begin{cases} 1, & \text{node } i, j \text{ belong to the same community} \\ 0, & \text{otherwise} \end{cases}$$

This study is based on the Louvain algorithm owing to its rapid convergence properties, high modularity and hierarchical partitioning. This algorithm starts by putting all the vertices of a network in distinct communities, one per node. It then sequentially sweeps over all the vertices in the inner loop. For each node $i$, the algorithm performs two calculations: (1) computes the modularity gain $\triangle Q$ when putting the node $i$ in the community of any neighbor $j$; (2) picks the neighbor $j$ that yields the largest gain in $\triangle Q$ and joins the corresponding community. This loop continues until no movement yields any further gains. At the end of this phase, the Louvain algorithm obtains the first level partitions. In the second step, these partitions become supervertices and the algorithm reconstructs the network by calculating the weight of the links between all the supervertices. Two supervertices are connected if there is at least one link between the vertices of the corresponding partitions, in which case the weight of the link between the two supervertices is the sum of the degrees from all the links between their corresponding partitions at

the lower level. These two steps of the algorithm are then repeated, yielding new hierarchical levels and supergraphs. The algorithm stops when communities become stable. The Louvain algorithm typically converges very quickly, and it can identify communities in just a few iterations. The Louvain algorithm was used to divide the functional brain networks.

### E. Community Selection

During the community detection, it is important to evaluate the best classification performance of functional brain networks at different scales. This study uses the Variation of Information (VI) and the Normalized Mutual Information (NMI) to evaluate the similarity of community structure in functional brain networks at different scales. They are simple theoretical information criteria used to compare two clusters based on the information exchange-loss and gain-between them. In this study, VI and NMI are introduced as the detection quantities of the community structure:

$$VI(C, C') = H(C) + H(C') - 2I(C, C')$$
$$NMI(C, C') = -2I(C, C')/(H(C) + H(C'))$$

The VI is equal to zero with the broadest range, which represents the most stable partition across different densities [32]. The greater value of NMI means that the more similarity exists between different communities. We can compare the performances of the community division between adjacent scales according to VI and NMI, and the most stable part of the community was identified as the ultimate community partition of the functional brain networks.

## IV. Results

### A. Functional Brain Networks

In this study, functional brain networks are constructed based on two different criteria for measuring the similarity of brain regions, as shown in Figure 2. In the functional brain network constructed by the DTW, the correlation between ROIs is expressed in the DTW values ranged between 0 and 1.4, which means that the distance between two unconnected brain region's time-series approaches around 1.4. In a word, when the DTW value tends to zero, correlation between the two brain regions is higher. On the contrary, when the DTW value tends towards 1.4, the similarity between the two brain regions is lower. In the functional brain network constructed by Pearson correlation, the correlation between two brain regions is expressed using a range from 0 to 1. The higher the correlation, the higher the similarity between the two brain regions. Using DTW as the measuring criteria of similarity can better describe the relationship between brain regions due to its broader scope. In order to analyze the functional brain network at multiple scales, we sparsed the structural connection matrix into a binarized and undirected network using different densities.As shown in Figure 3, We found that when the density level is small, the description of the link correlation is roughly consistent. However, there were more obvious differences between the two kinds of brain networks as the density increased.

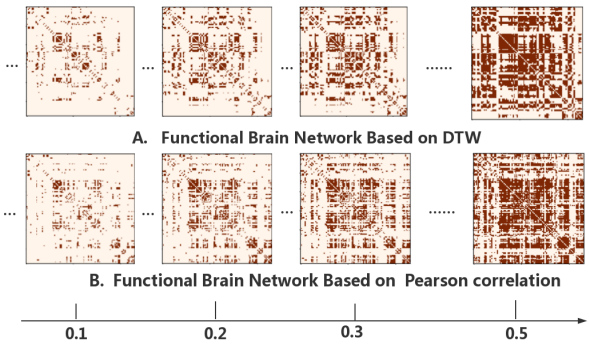


Fig. 3. Binary Brain Networks under tow standards with different densities.(A) represents the functional brain network based in the DTW; (B) denotes the functional brain network constructed by Pearson correlation. The value 0 and 1 respectively means the color white and red.

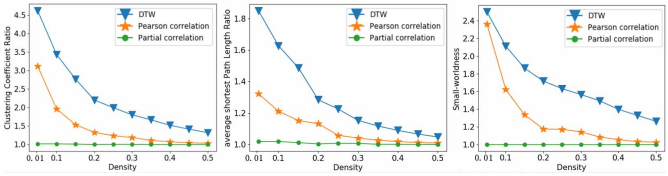


Fig. 4. The results of the network characteristics. A description of the clustering coefficient ratio, minimum path length ratio and small-worldness of brain networks, respectively constructed using DTW, Pearson correlation and Partial correlation is included. In brain networks based on the DTW, Pearson correlation, the clustering coefficient ratio, minimum path length ratio and small-worldness all decreased with an increase in the density value. In brain networks constructed using Partial correlation, the clustering coefficient ratio, minimum path length ratio and small-worldness were almost unchanged and approximately equal to 1.

### B. Characteristics of the Functional Brain Networks

We used different methods to measure the similarity between brain regions, that is, to establish the links of the brain network, so as to obtain different functional brain networks. The characteristics of the different brain networks are shown in Figure 4. We found that with an increase in density in the functional brain network based on Pearson correlation or DTW, and the values of the coefficients $\gamma$ and $\lambda$ decreased to about 1. When the $\lambda$ values of both networks tended to be one, the $\gamma$ value of the functional brain network constructed by DTW was higher than that based on Pearson correlation. Compared to the above two methods, the $\lambda$ values of the functional brain network constructed using Partial correlation approximated to 1, but the $\gamma$ was too small. Among the networks based on the three different methods, the small-worldness $\sigma$ value in network constructed using DTW was greater than that of the other two kinds of networks, which was the most conducive to our analysis of brain community structure. Furthermore, it is apparently unreasonable to construct functional brain networks based on Partial correlation because its $\sigma$ value close to 1.Therefore, we only consider using DTW and Pearson correlation to characterize node connections instead of the Partial correlation.

### C. Multiscale Community Detection

In general, when the modularity ranges from 0.3 to 0.8, it indicates that the network contains a community structure. Since the method in this study does not require the number of

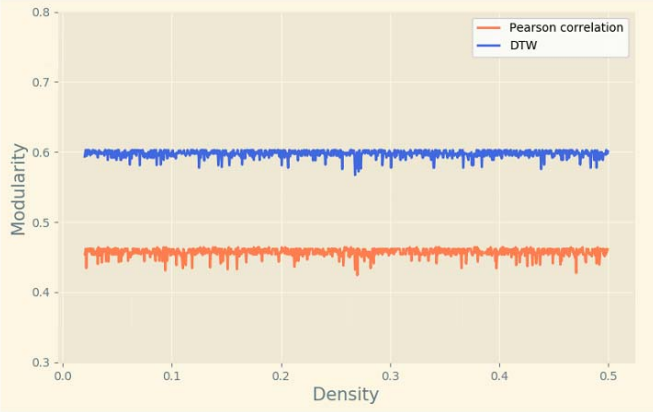


Fig. 5. Modularity of functional brain networks with different links. The blue line represents the modularity of the functional brain network based on the DTW; while the orange line denotes the modularity of the functional brain network constructed by Pearson correlation.

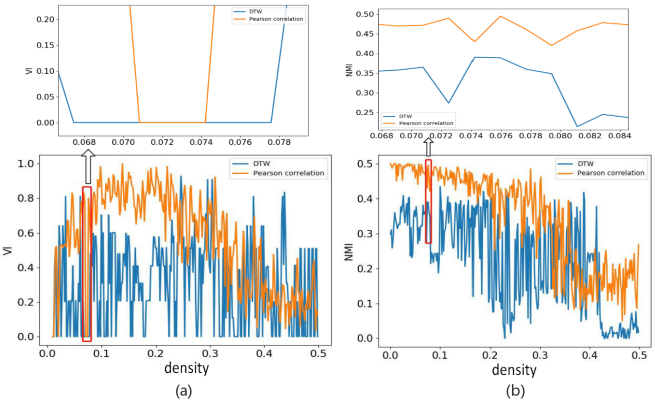


Fig. 6. Selection of the optimal partition for each kind of the functional brain network. (a) and (b) respectively illustrate VI, NMI values and corresponding to the density values in the functional brain network. Blue line shows the VI values and NMI values when different density values in functional brain network based on DTW, while orange line represents these in functional brain network constructed by Pearson correlation. When VI is zero and NMI is greater, the community structure is more stable, as marked in red.

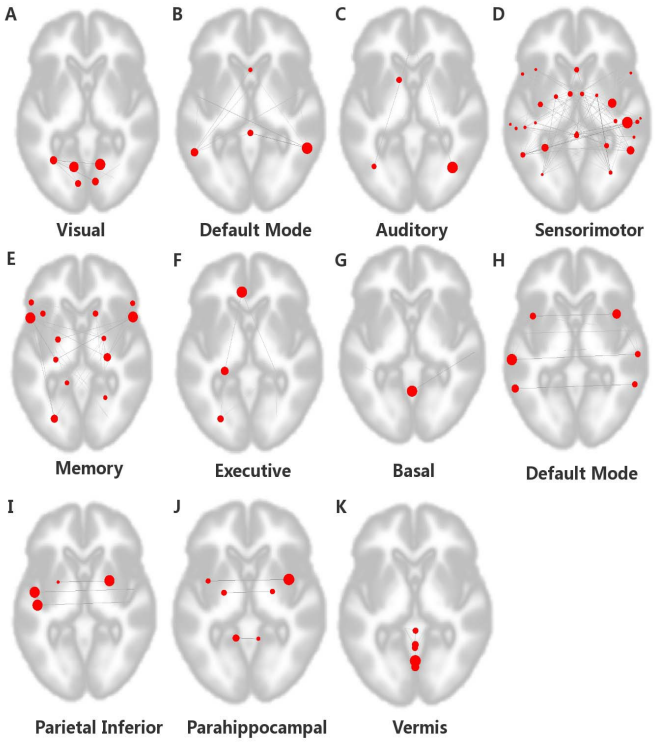


Fig. 7. Eleven largest mcommunities found by multiscale community detection in the resting state network constructed using DTW overlaid on an MRI brain template. The communities are named after corresponding functional networks previously identified by multivariate analysis of resting state fMRI data, or by the comprised anatomical districts.

clusters and other parameters in advance, it can be directly applied to the detection of functional brain networks. The experimental results are shown in Figure 5. For the functional brain network based on DTW, the modularity always fluctuates around 0.6; while the modularity of the functional brain network based on Pearson correlation always fluctuates around 0.45. Therefore, the modularity in our method is improved by 0.15. This is very helpful for us since it allows the discovery of communities in the functional brain network. However, as shown in Figure 5, we cannot observe the best community when only relying on modularity values. Thus, we introduced the VI and NMI as monitoring variables to examine the best community division by comparing the community structure between brain networks with adjacent densities. When the community structure of the brain network does not change, which means that the VI value is 0, the community structure is deemed stable. As shown in Figure 6(a) we found that the stability of both kinds of brain networks varies irregularly with the density. When the density value is between 0.068 and 0.0775, the social structure of the functional brain network based on DTW is the most stable. Combined with Figure 6(b), we chose the maximum value of NMI within this range and finally determined the optimal density value as 0.074. In the functional brain network constructed using Pearson correlation, the community structure is more stable when the density value ranges from 0.0705 to 0.074. Similar results have been obtained by applying this method to other data sets, as shown in the supplementary materials. In this case, the density value reaches 0.072 and the NMI value is greatest and the community structure is optimal. After determining the density, we repeated community detection 10000 times and finally obtain a single consensus community structure. 11 communities were discovered in the partition of the functional brain network based on DTW, and 15 communities based on Pearson correlations. The results of community detection in different functional brain networks are shown in Table 1.

we found that the 11 communities in the functional network constructed by DTW ranged in size from 4 to 28. The largest community consisted of 28 brain regions, including the precentral, postcentral, superior occipital gyrus, the supplementary motor area and so, which are related to the organizational and executive abilities of higher-level sports, as well as to higher-level mental activities such as empathy and problem-solving abilities. The second major community included the orbital part of the superior frontal gyrus, anterior cingulate gyrus and paracingulate gyrus, occipital gyrus, and hippocampus, which are mainly responsible for memory, as shown specifically in Figure 7. The brain networks based on Pearson

TABLE I
COMMUNITIES IN THE BRAIN FUNCTIONAL NETWORK

| Community | The brain regions contained in DTW brain network | Pearson brain network contains brain regions | nodes |
|---|---|---|---|
| 1 | Lingual, Occipital_Mid, Cuneus, Cerebelum_7b_L, Cerebelum_8 | Cingulum_Mid, Cingulum_Post, Hippocampus, ParaHippocampal, Amygdala, Occipital_Sup, Occipital_Mid, Parietal_Sup, Parietal_Inf, Cerebelum_7b_L, Cerebelum_8 | 9/21 |
| 2 | Frontal_Sup, Temporal_Inf, Cingulum_Ant | Lingual, Fusiform, Cingulu_Ant, Frontal_Sup | 6/8 |
| 3 | Caudate_L, Frontal_Sup_Medial, Cerebelum_Crus1, Cerebelum_Crus2 | Caudate_L, Frontal_Sup_Medial, Temporal_Pole_Sup, Cerebelum_Crus1, Cerebelum_Crus2 | 7/9 |
| 4 | Precentral, Postcentral, Caudate_R, Occipital_Sup, Cingulum_Mid, Frontal_Mid, Supp_Motor_Area_L, Cingulum_Post, Parietal_Inf, Rolandic_oper, Pallidum, Paracentral_L, Parietal_Sup,Temporal_Pole_Sup, Frontal_Inf_Oper, Vermis_1_2 | Precentral, Rolandic_Oper, Caudate_R, Supp_Motor_Area_L, Frontal_Inf_Oper, Insula, Postcentral, Paracentral_L, Angular, Frontal_Mid, Pallidum, SupraMarginal, Vermis_1_2 | 28/23 |
| 5 | Frontal_Sup_Orb, Occipital_Inf_L, Hippocampus, Frontal_Mid_Orb, Frontal_Inf_Tri, Frontal_Inf_Orb, Olfactory_L, Amygdala, Cerebelum_4_5, Cerebelum_6, Putamen_R, Paracentral_Lobule | Frontal_Sup_Orb, Frontal_Mid_Orb, Frontal_Inf_Tri, Frontal_Inf_Orb, Occipital_Inf, Olfactory, emporal_Inf, Cerebelum_Crus2, Cerebelum_6, Vermis_6, Cerebelum_4_5, Paracentral_R, Paracentral_Lobule | 21/24 |
| 6 | Fusiform, Calcarine, Cerebelum_10, Supp_Motor_Area_R | Cuneus, Calcarine, Temporal_Sup, Supp_Motor_Area_R | 7/7 |
| 7 | Precuneus, Temporal_Sup | Thalamus, Rectus, Temporal_Mid, Temporal_Pole_Mid, Cerebelum_10 | 4 /10 |
| 8 | Thalamus, Rectus, Temporal_Mid, Temporal_Pole_Mid, Paracentral_R | Putamen, Heschl, Precuneus | 9/6 |
| 9 | Putamen_L, Heschl, Angular_L, Supramarginal, Occipital_Inf_R, Olfactory_R | Cerebelum_9, Vermis_4_5 | 8/3 |
| 10 | ParaHippocampal, Insula, Cerebelum_9, Angular_R | Cerebelum_3 | 7/2 |
| 11 | Vermis_3, Vermis_4_5, Vermis_6, Vermis_7, Vermis_8, Vermis_9, Vermis_10, Cerebelum_3, Cerebelum_7b_R | Vermis_3, Cerebelum_7b_R | 10 /2 |
| 12 | NALL | Vermis_7 | 0/1 |
| 13 | NALL | Vermis_8 | 0/1 |
| 14 | NALL | Vermis_9 | 0/1 |
| 15 | NALL | Vermis_10 | 0/1 |

Table 1. The functional brain networks constructed using DTW and Pearson correlation are respectively referred as DTW Network and Pearson correlation Network in this table. Because the brain is symmetrical, each brain region is divided into two parts, such as Lingual includes left Lingual and right lingual, but besides Vermis_1_2, Vermis_3, Vermis_4_5, Vermis_6, Vermis_7, Vermis_8, Vermis_9, Vermis_10. The suffix "_L" denotes the left part of the brain and the suffix "_R" denotes the right part of the brain. Otherwise, there are two left and right parts of the brain area.

correlation indicated 15 communities, ranging in size from 1 to 24. The largest community contained 24 brain regions, including the precentral, supplementary motor area and so on, which are related to the organization and execution ability in advanced sports. The second community is responsible for memory work and has 22 brain regions in total, consisting respectively of the orbital part of the superior frontal gyrus, the orbital part of the middle frontal gyrus, the triangle part of the inferior frontal gyrus etc. Although the subnetworks in the two methods contained different numbers of brain regions, the importance of the subnetworks in brain activity was not changed. Whether constructed with DTW or Pearson correlations, the results of multiscale community detection based on the Louvain algorithm showed that most of the functional partitions are consistent. All subnetworks are composed of the visual network, auditory network, motor network, default mode network and executive-working memory-related network. However, the functional brain network based on Pearson correlations is less sensitive to the cerebellum than that with DTW, and some cerebellar areas are regarded as an independent component. More importantly, we found that the inferior parietal lobe was functionally connected with the putamen and Heschl's gyrus in addition to the angular gyrus and supramarginal gyrus.

## V. DISCUSSION

Applying a multiscale community detection approach to functional brain network analysis based on DTW, we found that the main functional sub-networks included the visual network, auditory network, motor network, default mode network and executive network. The components of these functional brain networks are roughly the same as those of previous findings. Besides, compared with the functional brain network constructed using Pearson correlation, there are some differences in the discovery of cerebellar function. Parts of the cerebellum are closely related to brain activities in

the functional brain network based on DTW. For example, Vermis_1_ 2 in the cerebellum affect motor function. Besides, the cerebellum does not only have an important impact on human memory function, but also controls human linguistic abilities [33], [34]. Therefore, we can conclude that the brain and cerebellum are anatomically separated, but functionally interact and cooperate with each other. More importantly, we found a new inferior parietal network that is functionally connected with the putamen and Heschl's gyrus [35] in addition to the angular gyrus and the supramarginal gyrus.

### A. Construction of Functional Brain Networks

Constructing functional brain networks close to our human brain is very important for researching human brain. In general, using Pearson correlation and Partial correlation to analyze the correlation between different brain regions depends on the synchronization of signals of fMRI time series, which means that the activities between brain regions are consistent. In fact, information in the brain is transmitted to each other according to a certain direction [36]. The transmission of this information makes one brain region influence information in another brain region. Therefore, there are synchronizations and asynchronisms in brain activity. Brain functional connectivity describes the temporal correlation of spatially unrelated brain regions when some neurophysiological events occur at a certain time. Therefore, using Pearson correlation or Partial correlation to describe the correlation between brain regions ignores the effect of information transmission between brain regions.

Using DTW to estimate similarity between brain regions can simultaneously capture synchronization and asynchronization correlation information in fMRI time series. Originally, DTW was proposed to compare the similarity in time series based on the synchronization and asynchronism of the time series, and it has been well used in speech recognition. DTW synthesizes comparison sequences in a path-ordered way to express their similarities more accurately. This method has been widely and successfully used in dynamic time series, image and text similarity comparison [37]. This study applies this method to distinguish the similarity of fMRI time series and reports new findings in functional brain networks based on DTW including the description of similarities between brain regions, which can describe the correlation between brain regions in detail. Therefore, using DTW to construct functional brain networks is conducive to the discovery of changes in brain structure, which is of great significance to the study of brain diseases.

### B. Analysis of the Network Characteristics

There are two basic organizational principles in functional brain networks, namely functional differentiation and functional integration. Functional differentiation [38] refers to the high probability of connecting neighboring neurons in a spatial distance to each other and forming units with certain independent functions. The clustering coefficient of the brain neural network can reflect this characteristic [39]. Functional integration refers to the low probability of interconnection between distant neurons in space, which can be reflected by the average shortest path length of the brain network [40]. Long axonal projections require more material and energy costs, so the number of neural connections between different brain functional units is less than that within the unit. However, a small amount of long axonal projections is enough to make brain neural connection networks have an average shortest path length, so that the brain achieves an "economic" mode that is both holistic and locally focused [41]. Therefore, the clustering coefficients of the brain network reflect the functional differentiation mechanism of the cerebral cortex, which expresses the tightness of the connections between neurons in the functional areas of the local brain. The average shortest path length can characterize whether the brain's energy and material consumption is "economic" during the execution of cognitive tasks. Our results show that the functional brain network has a large clustering coefficient and small average shortest path length, which proves that the brain network has a "small world" effect.

Using graph theoretical approaches to the analysis of complex networks can provide a powerful new way of quantifying the brain's functional systems, and small-world plays a key role in studying complex networks [42]. The small-world network means the network with shorter average path length and higher clustering coefficients, so it is strongly related with definition of nodes and links. But noise and common sources can lead to the estimate distortions about links, which affects the small-world effect of functional brain network. We should have efforts to quantify functional networks' information transfer efficiency or reliability by capturing physiological information transfer and processing. The proposed method in this study is not only insensitive to noise but can capture physiological information transfer. Therefore, the small world of functional brain networks using DTW is closer to the real human brain. Moreover, compared with functional brain networks constructed by Pearson correlation and Partial correlation, using DTW to construct functional brain network can better highlight the characteristics of the brain network. Previous studies have shown that the "small world" effect of brain networks has not changed in normal people or in patients with brain conditions, such as schizophrenia, childhood attention deficit hyperactivity disorder, Alzheimer's disease and multiple sclerosis [43], [44]. Therefore, we believe that the construction of a functional brain network by DTW is more helpful for the analysis of brain diseases due to its more obvious "small world" effect, and the current experimental results also prove this point. However, there are some inherent limitations about small-worldness beyond the possible effects of measurement noise, such as comparison with "equivalent random networks" and possible effects of the spatial limitations on small-worldness. Unfortunately, these problems are unavoidable at present, and will be further explored in future research.

### C. Multiscale Community Detection

The community organization of large-scale human functional networks appears to reflect the underlying neurobiological mechanisms, and variations in the community structure

can signal significant changes in the brain's functional capacities [45]. The study has proven that an individual's functional brain connectivity profile is both unique and reliable, similarly to a fingerprint. The intra-individual reliability observed here suggests that the general blueprint may be shared, but the functional organization within individual subjects is idiosyncratic [46]. Therefore, identification of each human brain network density has been extremely fruitful for studying the organizing principles of individuals. In this study, we detected the community structure at different densities of functional brain networks. Through the analysis of modularity, VI and NMI, we detected the best community structure of each subject and determined the subject's brain network density.

This method has been applied to the two kinds of functional brain networks constructed by DTW and Pearson correlation respectively. In the two kinds of brain networks, we also found seven basic functional brain networks, including the visual network, auditory network, motor network, default mode network and executive-working memory-related network. At the same time, our findings include Vermis network because the 116 nodes defined in this paper contain cerebellum. In addition, Parahippocampal and Parietal Inferior are derived from Seven Basic Networks, but they are important for studying some diseases. Parahippocampal is closely related to memory network, which has great significance on studying cognitive impairment and Alzheimer's disease [47]. Inferior parietal network is bound up with executive-working network, including putamen and Heschl's gyrus. More importantly, we also report new findings describing the real structure of the brain more accurately.

From a structural and functional point of view, each community is independent of the main executor of a function, and the functions of each community are coordinated to form a whole, jointly serving the brain integration function. We found that the brain and cerebellum interact with each other and accomplish certain cognitive functions together. Besides, there are some new findings in the inferior parietal network. Previous studies have shown that the inferior parietal network often includes the angular gyrus and the supramarginal gyrus. Additionally, we found that this network is also related with the putamen and Heschl's gyrus. The inferior parietal network is mainly responsible for the functions of body sensation, taste and touch [48]. If the inferior parietal network is damaged, there is usually abnormal sensation or sensory disturbances in the cerebral cortex, apraxia, dyslexia, ipsilateral isotropic lower quadrant blindness, spatial localization disorder and physical atrophy. Studies have shown that damage to the putamen is closely related to such lesions as hemianesthesia and hemianopia [49]. Damage to Heschl's gyrus also causes hemianopia and disorientation [50]. Therefore, the putamen and Heschl's gyrus both have a certain connection with respect to human sensations. It is also reasonable to attribute the putamen and Heschl's gyrus to the inferior parietal network, which is significant for the studying of human sensation.

Our findings showed that the community division is not consistent with previous studies, in terms of number and size of the communities in functional brain networks [51]. Although there is no fixed division of the brain regions, it is still reasonable in terms of function and structure. A multiscale community observation is not only helpful for us to find the best community structure in different individuals, but also confirms the scale of each subject. Our study suggested that the individual differences could be explored by our proposed method, such as intelligence, mental illness and so on.

## VI. Conclusion

According to the characteristics of the fMRI time series, this study applies the DTW technique to construct functional brain networks. Our experiments showed that the functional brain networks constructed by DTW have a more obvious "small-world" effect and are closer to the human brain. Secondly, we used modularity, VI and NMI as monitoring variables for the community structure, which not only helped us find the best community structure in multiscale functional brain networks, but also determined the threshold. This is of great significance for exploring a subject's functional brain networks, such as intelligence and in mental disorders. Through our proposed approach, we not only accurately observed the important elements in the seven basic functional communities, but also discovered the other components in the inferior parietal network except for the angular gyrus and the supramarginal gyrus. This also fully proves the feasibility of the method in this study. In addition, this study reveals the motor state of the human brain involved in functional activities and provides an effective method for the study of human brain pathologies.

## References

[1] A. R. Anwar *et al.*, "Complex network analysis of resting-state fMRI of the brain," in *Proc. 38th Annu. Int. Conf. IEEE Eng. Med. Biol. Soc. (EMBC)*, Aug. 2016, pp. 3598–3601.
[2] O. Sporns and R. F. Betzel, "Modular brain networks," *Annu. Rev. Psychol.*, vol. 67, no. 1, pp. 613–640, 2016.
[3] M. J. Lowe, B. J. Mock, and J. A. Sorenson, "Functional connectivity in single and multislice echoplanar imaging using resting-state fluctuations," *Neuroimage*, vol. 7, no. 2, pp. 119–132, 1998.
[4] D. Cordes *et al.*, "Frequencies contributing to functional connectivity in the cerebral cortex in 'resting-state' data," *Amer. J. Neuroradiol.*, vol. 22, no. 7, pp. 1326–1333, 2001.
[5] M. Hampson, B. S. Peterson, P. Skudlarski, J. C. Gatenby, and J. C. Gore, "Detection of functional connectivity using temporal correlations in MR images," *Hum. Brain Mapping*, vol. 15, no. 4, pp. 247–262, 2002.
[6] O. Sporns, "Contributions and challenges for network models in cognitive neuroscience," *Nature Neurosci.*, vol. 17, no. 5, pp. 652–660, 2014.
[7] C. E. Forbes, R. Amey, A. B. Magerman, K. Duran, and M. Liu, "Stereotype-based stressors facilitate emotional memory neural network connectivity and encoding of negative information to degrade math self-perceptions among women," *Social Cogn. Affect. Neurosci.*, vol. 13, no. 7, pp. 719–740, 2018.
[8] Q. Yu *et al.*, "Application of graph theory to assess static and dynamic brain connectivity: Approaches for building brain graphs," *Proc. IEEE*, vol. 106, no. 5, pp. 886–906, May 2018.
[9] S. M. Smith, "The future of FMRI connectivity," *Neuroimage*, vol. 62, no. 2, pp. 1257–1266, 2012.
[10] P. P. Broca *et al.*, "Functional neuroimaging information: A case for neuro exceptionalism," *AJOB Neurosci.*, vol. 9, no. 1, pp. W1–W20, 2018.
[11] S. M. Smith *et al.*, "Functional connectomics from resting-state fMRI," *Trends Cognit. Sci.*, vol. 17, no. 12, pp. 666–682, 2013.
[12] F. M. Krienen, *Large-Scale Networks in the Human Brain Revealed by Functional Connectivity MRI*. Cambridge, MA, USA: Harvard Univ., 2013.

[13] Y. Zhou, L. Qiao, W. Li, L. Zhang, and D. Shen, "Simultaneous estimation of low- and high-order functional connectivity for identifying mild cognitive impairment," *Frontiers Neuroinform.*, vol. 12, pp. 1–8, 2018.

[14] X. Geng, J. Xu, B. Liu, and Y. Shi, "Multivariate classification of major depressive disorder using the effective connectivity and functional connectivity," *Frontiers Neurosci.*, vol. 12, p. 38, Feb. 2018.

[15] H. Zhang *et al.*, "Topographical information-based high-order functional connectivity and its application in abnormality detection for mild cognitive impairment," *J. Alzheimer's Disease*, vol. 54, no. 3, pp. 1095–1112, Oct. 2016.

[16] X. Chen *et al.*, "High-order resting-state functional connectivity network for MCI classification," *Hum. Brain Mapping*, vol. 37, no. 9, pp. 3282–3296, 2016.

[17] X. Huang, Y. Song, and H. Lu, "Detecting community structure of resting-state functional network based on optimizing modularity by genetic algorithm," *J. Jiangsu Univ. Sci. Technol. (Natural Sci. Ed.)*, vol. 31, no. 6, pp. 787–794, 2017.

[18] E. S. Finn *et al.*, "Functional connectome fingerprinting: Identifying individuals using patterns of brain connectivity," *Nature Neurosci.*, vol. 18, no. 11, pp. 1664–1671, 2015.

[19] X. Wang, Y. Ren, and W. Zhang, "Depression disorder classification of fMRI data using sparse low-rank functional brain network and graph-based features," *Comput. Math. Methods Med.*, vol. 2017, Apr. 2017, Art. no. 3609821.

[20] M. Liu, C.-C. Kuo, and A. W. L. Chiu, "Statistical threshold for nonlinear granger causality in motor intention analysis," in *Proc. Annu. Int. Conf. IEEE Eng. Med. Biol. Soc.*, Aug./Sep. 2011, pp. 5036–5039.

[21] N. Jrad *et al.*, "Automatic detection and classification of high-frequency oscillations in depth-EEG signals," *IEEE Eng. Med. Biol.*, vol. 64, no. 9, pp. 2230–2240, Sep. 2017.

[22] C. Nicolini, C. Bordier, and A. Bifone, "Community detection in weighted brain connectivity networks beyond the resolution limit," *Neuroimage*, vol. 146, pp. 28–39, Feb. 2017.

[23] M. Dinov, R. Lorenz, G. Scott, D. J. Sharp, E. D. Fagerholm, and R. Leech, "Novel modeling of task vs. rest brain state predictability using a dynamic time warping spectrum: Comparisons and contrasts with other standard measures of brain dynamics," *Frontiers Comput. Neurosci.*, vol. 10, p. 46, May 2016.

[24] R. J. Meszlényi, P. Hermann, K. Buza, V. Gál, and Z. Vidnyánszky, "Resting state fMRI functional connectivity analysis using dynamic time warping," *Frontiers Neurosci.*, vol. 11, p. 75, Feb. 2017.

[25] M. Meilă, "Comparing clusterings by the variation of information," in *Learning Theory and Kernel Machines*. Berlin, Germany: Springer, 2003, pp. 173–187.

[26] P. A. Estévez, M. Tesmer, C. A. Perez, and J. M. Zurada, "Normalized mutual information feature selection," *IEEE Trans. Neural Netw.*, vol. 20, no. 2, pp. 189–201, Feb. 2009.

[27] X. Liao, A. V. Vasilakos, and Y. He, "Small-world human brain networks: Perspectives and challenges," *Neurosci. Biobehav. Rev.*, vol. 77, pp. 286–300, Jun. 2017.

[28] N. Tzourio-Mazoyer *et al.*, "Automated anatomical labeling of activations in SPM using a macroscopic anatomical parcellation of the MNI MRI single-subject brain," *NeuroImage*, vol. 15, no. 1, pp. 273–289, 2002.

[29] V. D. Blondel, J.-L. Guillaume, R. Lambiotte, and E. Lefebvre, "Fast unfolding of communities in large networks," *J. Stat. Mech., Theory Exp.*, vol. 2008, no. 10, 2008, Art. no. P10008.

[30] D. S. Bassett and E. D. Bullmore, "Small-world brain networks," *Neuroscientist*, vol. 12, no. 6, pp. 512–523, 2006.

[31] M. E. J. Newman and M. Girvan, "Finding and evaluating community structure in networks," *Phys. Rev. E, Stat. Phys. Plasmas Fluids Relat. Interdiscip. Top.*, vol. 69, Feb. 2004, Art. no. 026113.

[32] Y. He *et al.*, "Reconfiguration of cortical networks in MDD uncovered by multiscale community detection with fMRI," *Cerebral Cortex*, vol. 28, no. 4, pp. 1383–1395, 2018.

[33] R. L. Buckner, "The cerebellum and cognitive function: 25 years of insight from anatomy and neuroimaging," *Neuron*, vol. 80, no. 3, pp. 807–815, 2013.

[34] C. C. Bell, V. Han, and N. B. Sawtell, "Cerebellum-like structures and their implications for cerebellar function," *Annu. Rev. Neurosci.*, vol. 31, no. 31, pp. 1–24, 2008.

[35] S. Zhang and C.-S. R. Li, "Functional clustering of the human inferior parietal lobule by whole-brain connectivity mapping of resting-state functional magnetic resonance imaging signals," *Brain Connectivity*, vol. 4, no. 1, pp. 53–69, 2014.

[36] J. Xu *et al.*, "Heritability of the effective connectivity in the resting-state default mode network," *Cerebral Cortex*, vol. 27, no. 12, pp. 5626–5634, 2016.

[37] Y. Chen, B. Hu, E. Keogh, and G. E. A. P. A. Batista, "DTW-D: Time series semi-supervised learning from a single example," in *Proc. ACM SIGKDD Int. Conf. Knowl. Discovery Data Mining*, 2013, pp. 383–391.

[38] S.-W. Hou *et al.*, "Functional integration of newly generated neurons into striatum after cerebral ischemia in the adult rat brain," *Stroke*, vol. 39, no. 10, pp. 2837–2844, 2008.

[39] C. Li, H. Wang, W. De Haan, C. J. Stam, and P. Van Mieghem, "The correlation of metrics in complex networks with applications in functional brain networks," *J. Stat. Mech., Theory Exp.*, vol. 2011, no. 11, 2011, Art. no. P11018.

[40] M. Cao *et al.*, "Early development of functional network segregation revealed by connectomic analysis of the preterm human brain," *Cerebral Cortex*, vol. 27, no. 3, pp. 1949–1963, 2017.

[41] Q. K. Telesford, K. E. Joyce, S. Hayasaka, J. H. Burdette, and P. J. Laurienti, "The ubiquity of small-world networks," *Brain Connectivity*, vol. 1, no. 5, pp. 367–375, 2011.

[42] D. Papo, M. Zanin, J. H. Martínez, and J. M. Buldú, "Beware of the small-world neuroscientist!" *Frontiers Hum. Neurosci.*, vol. 10, p. 96, Mar. 2016.

[43] R. Russo, H. J. Herrmann, and L. de Arcangelis, "Brain modularity controls the critical behavior of spontaneous activity," *Sci. Rep.*, vol. 4, Mar. 2014, Art. no. 4312.

[44] R. L. Buckner, F. M. Krienen, A. Castellanos, J. C. Diaz, and B. T. Yeo, "The organization of the human cerebellum estimated by intrinsic functional connectivity," *J. Neurophysiol.*, vol. 106, no. 5, pp. 2322–2345, 2011.

[45] M. A. Bertolero, B. T. Yeo, and M. D'Esposito, "The modular and integrative functional architecture of the human brain," *Proc. Nat. Acad. Sci. USA*, vol. 112, no. 49, pp. E6798–E6807, 2015.

[46] M. Liu, R. C. Amey, and C. E. Forbes, "On the role of situational stressors in the disruption of global neural network stability during problem solving," *J. Cognit. Neurosci.*, vol. 29, no. 12, pp. 2037–2053, 2017.

[47] T. W. Mitchell *et al.*, "Parahippocampal tau pathology in healthy aging, mild cognitive impairment, and early Alzheimer's disease," *Ann. Neurol.*, vol. 51, no. 2, pp. 182–189, 2002.

[48] N. A. Crossley *et al.*, "Cognitive relevance of the community structure of the human brain functional coactivation network," *Proc. Nat. Acad. Sci. USA*, vol. 110, no. 28, pp. 11583–11588, 2013.

[49] D. M. Clower, R. A. West, J. C. Lynch, and P. L. Strick, "The inferior parietal lobule is the target of output from the superior colliculus, hippocampus, and cerebellum," *J. Neurosci. Off. J. Soc. Neuroscience*, vol. 21, no. 16, pp. 6283–6291, 2001.

[50] E. D. Playford, I. H. Jenkins, R. E. Passingham, J. Nutt, R. S. J. Frackowiak, and D. J. Brooks, "Impaired mesial frontal and putamen activation in Parkinson's disease: A positron emission tomography study," *Ann. Neurol.*, vol. 32, no. 2, pp. 151–161, 1992.

[51] K. M. Smith *et al.*, "Morphometric differences in the Heschl's gyrus of hearing impaired and normal hearing infants," *Cerebral Cortex*, vol. 21, no. 5, pp. 991–998, 2011.